Estimation of Operational Intention and Personal Adaptation in Power Assist System

2013

Master of Engineering

Department of Mechanical Engineering

MOHD HAZWAN BIN ABD LATIF

093247

Toyohashi University of Technology

2014年3月14日

機械工学専攻		学籍番号	093247
申請者氏名	MOHD HAZWAN BIN ABD LATIF		

指導教員氏名	寺嶋一彦 教授

論 文 要 旨 (修士)

論文題目	Estimation of Operational Intention and Personal Adaptation in Power Assist System (パワーアシスト駆動の操作意図推定と個人適応)

(要旨 1,000字程度)

近年，出生数の低下と医療技術の発展による平均寿命の伸長から，超高齢化社会へと移行が進んでいる．これに伴い，若年世代の介護者の低下を招き，老老介護という介護形態が今後主流となると予想される．そのため，肉体的負担の大きい介護を支援する，福祉支援機器の開発が注目されている．その一例としてパワーアシスト技術が挙げられるが，本研究では，狭い室内などで自由に方向転換が可能な全方向移動ベッド（以下OMBと呼ぶ）に応用することで，介護者への負担低減を目指している．

全方向に移動するベッドにパワーアシストシステムを組み込んだ場合，動作の自由度から人間が意図した方向にパワーアシスト動作しないという問題が発生した．そのため従来研究では，ファジィ推論による方向推論を用いて操作性の向上を図った．その方法として，介助者の力の加え方の傾向からルールを作成し，そのルールとファジィパラメータからOMBの動作を決定した．

しかし，操作者が変わった場合，ファジィパラメータの再チューニングを行う必要があり，そのチューニングには多大な時間を要した．従って，本研究では，ファジィパラメータの再チューニングを自動化する目的で，ニューロ・ファジィをパワーアシストシステムに導入することを行った．ニューロ・ファジィは様々な手法が提案されているが，本研究ではANFIS(Adaptive-Network-Based Fuzzy Inference System)を用いる．ANFISは教師信号と実際に加えた入力からニューラルネットワークを用いて，ファジィパラメータの自動チューニングを行う．教師信号は人間の行きたい方向や動作方法からなる人間の意思データである．

以上より，上記の方向推論システムを構築し，ファジィパラメータの自動チューニングを行った．その結果，シミュレーション上に操作者個人の意図に沿うようにOMBをパワーアシスト動作をさせることが可能となるファジィパラメータを，短時間で導出することが可能となった．

Estimation of Operational Intention and Personal Adaptation in Power Assist System

MOHD HAZWAN BIN ABD LATIF

Department of Mechanical Engineering, Toyohashi University of Technology

Mar 2014

ABSTRACT

In recent years, social problems of elderly society such as the decreasing number of care-workers and heavy work of nurses have been increased. Especially, transferring of bed in hospital requires two nurses and the task is heavy and difficult. Therefore, power assist system is one of the effective solution and it is possible to reduce the number of nurses for operation from two person to one. In this study, the power assist system is applied to an Omnidirectional Mobile Bed (OMB), which can move in any directions and less movement is required to change direction, very advantageous in narrow spaces.

The goal of this study is to provide a nurse with power assist system that can help to move easily an OMB in narrow and crowded spaces in hospital. When the power assist system was installed to the OMB, there was a problem that the OMB did not move in the intended direction of the operator. Therefore, improvement of the operability was attempted by using direction reasoning by fuzzy reasoning. In this method, the rules are designed by how the force is applied by the operator, and the operation of the OMB is determined by the fuzzy ruled and fuzzy parameters.

However, when the operator is changed, it is necessary to tune the fuzzy parameters according to operator ' s parameters characteristics. As the tuning by trial and error takes a long time, in this paper, the fuzzy parameters are automatically tuned by using a neuro-fuzzy system ANFIS (Adaptive-Network-Based Fuzzy Inference System). The fuzzy parameters are auto-tuned by ANFIS by using teaching signals and input of the operator. The teaching signal is the data of the operator ' s intended direction of movement. The simulation results shows that there are improvement of operability of power assist after the tuning process for three opearators.

Finally, the effectiveness of the proposal approach is demonstrated through experiments.

Keywords: Omni-directional robot, nursing robot, power assist system, robotic-bed

Table of Contents

Chapter 1

General Introduction

1.1 Background

In recent years, due to the decrease of the birth rate and the development of medical technology, the proportion of elderly people every year is increasing. In year 2007, the aged population rate exceeds 21% and elderly care workers have become a social problem because of lack of young workers [1]. By 2035 it is expected that aged population will increase to 33%, and will increase in the future as shown in Fig 1.1. In addition, according to the government's announcement, the ratio of person with disabilities is about 6% of the total population [3]. This means that every four of ten persons will need assistance from care workers and nurses in hospital in their daily life.

In welfare facilities, it is reported that wheelchairs and beds are preferred than portable lifts or ceiling lifts on transferring the residents, because it is less time consuming and less danger of dropping a resident. Transfer of bed requires two workers and the operation to make bed transfer is difficult and heavy task. A survey reported that due to heavy workload in welfare

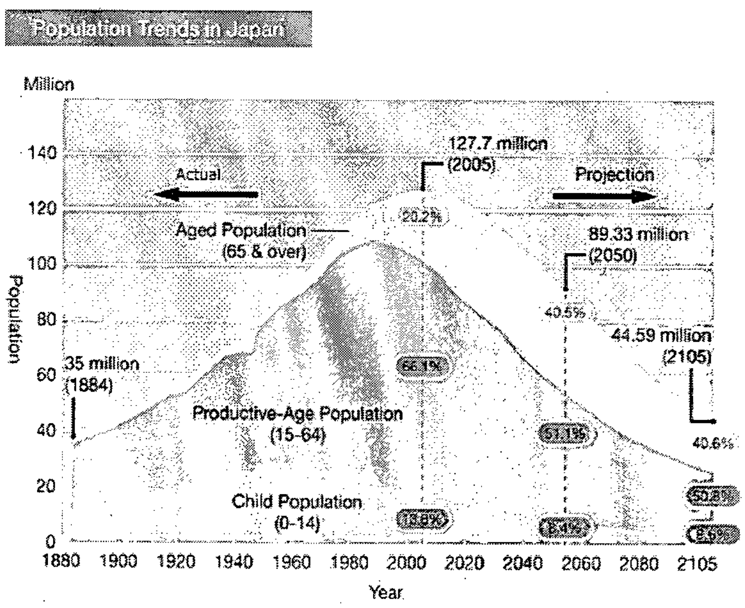

Fig. 1.1 Population trends in Japan

facility, musculoskeletal disorders have been increasing among care workers [4].

Therefore, in the medical welfare field, the application of advance technology in industrial sector to welfare support is highly expected. One of them is, the application of power assist technology on electric wheelchair which able to support heavy corporal burden of transferring task. In addition, recently, various supporting devices have been developed, especially omni-directional mobile robot to offer high mobility and independence for the user to enhance their quality of life .

The combination of power assist system and omni-directional robot is undoubtedly would be able to support the heavy workload and help reducing the mental burden of care workers, and is highly desirable.

1.2 Related researches

An omni-directional robot is highly maneuverable in narrow or crowded areas such as residences, offices and hospitals.. There are numerous researches and commercial electric wheelchairs and transferring robots that have been taking place in recent years. In omni-directional robot it began with the research about special wheels such as mecanum wheels [27], ball wheels [13], omni-disks [25] and omni-wheels [26].

Matsushita Electric Works have developed an Omni-directional Cart with Power-assist System, which the length is bigger than the width. They report problems with lateral motion when the length of the cart is very long. They have considered about turning, but for case of rotation over the center of gravity it is still unsolved problem[16]_[17]. Airtrax Corp. developed an omni-directional forklift by using mecanum wheels which improve workability in crowded area and reduce the work hours [14]. Yamaha Motor Co. Ltd have developed several type of electric wheelchairs with Power-assist System, which the attendant can easily push the wheelchair by small force and the passenger also can operate the wheelchair as manual wheelchair by using

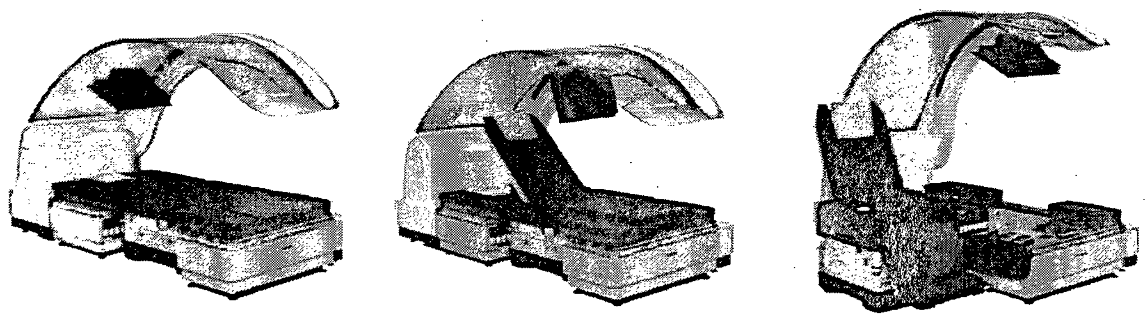

Bed mode Shown with the back rest up Wheelchair separated from the bed

Fig. 1.2 Robotic bed by Panasonic Corp.

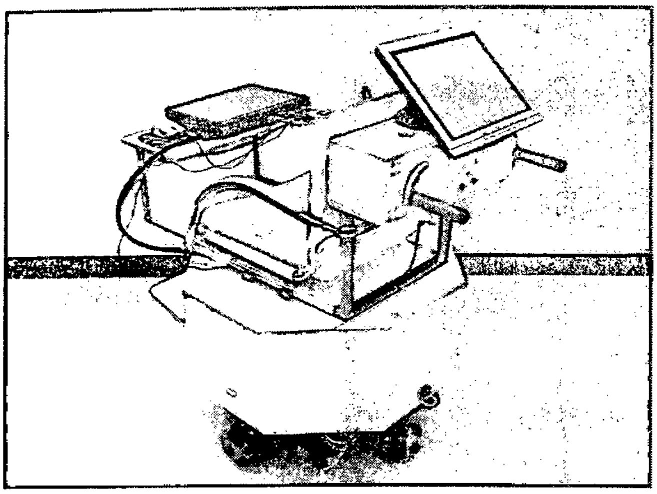

Fig. 1.3 Omni-directional wheelchair (OMW)

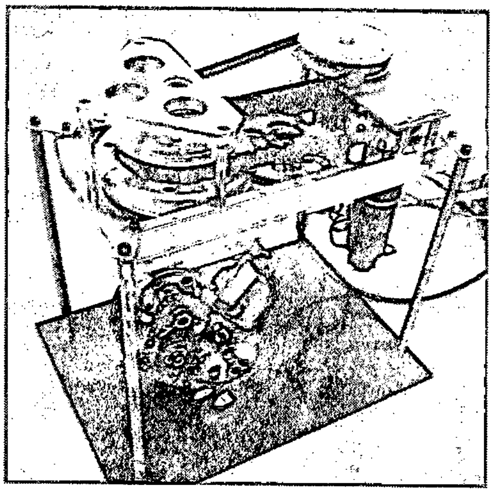

Fig. 1.4 DDSS unit

handrim with supported by motor unit called JW-2 [18]. Panasonic Corp. have developed a robotics bed as shown in Fig. 1.2 which a part of the bed can transform automatically to an omni-directional wheelchair, which can be operated easily in small space and patient does not need to get off from the bed to move to another place [6],[7].

In author's laboratory, Ohno constructed a caster-drive wheel using a Differential-Drive Steering System (DDSS) as shown in Fig. 1.4 to improve the ride comfort, vibration suppression, slippage reduction and ability to surmount different in level [8]–[11]. Ueno have applied six degree of freedom force sensor and DDSS to Omni-directional Mobile Robot and Omni-directional Mobile Bed. Both robots can be operated by power assist system for helper and joystick for patient [11]. Nishizaka applied Fuzzy Reasoning to improve the operability of the power assist handle in forward-backward and lateral direction, and rotation on gravity center motion [9]. Regarding the change of operationality when operator is changed, Watanabe estimated velocity and input force of operator and constructed stable system for OMW in Fig. 1.3 even in running condition by adjusting the time constant and gain. Furthermore, the author also developed a skill-assist system that estimate the skill of the operator from standard deviation of the velocity of wheels, and also the system reduce the skill-assist when correspond to skilled operator [10]. Juan and Kitamura improved the operability of power assist system of OMW by using the Adaptive Neuro-Fuzzy System and input data of operator to tune the parameters according to the operator's tendency [28],[29].

Other researches in author's laboratory are Kobayashi used ultrasonic sensor and infrared sensor in detection of obstacles and convert the sensor information to force-feedback of haptick joystick [20]. Kondo used laser range sensor and by using information of distant and direction of obstacle, the joystick not only give the feedback force but also lead the operator to safe direction [23].

1.3 Problems and Research purpose

In author's laboratory, the OMB is developed with operated by power assist system as mentioned in previous section. The OMB's size is larger with rectangle-shaped compared to OMW or other conventional electric wheelchairs, so it is difficult to operate. Therefore, the purpose of this research is to improve the operability of the power-assist system of OMB by using a neuro-fuzzy system that able to tune the fuzzy parameters automatically by using the input data of the operator.

1.4 Outline of this thesis

This thesis presents the improvement of the operation of an omni-directional mobile bed (OMB) in power assist. In Chapter 1 presents the background, related researches inside and outside author's laboratory, problems and purpose as well as outline of this thesis. In Chapter 2 describes the mechanism of DDSS, structure of OMB, the hardwares and kinematic model. In Chapter 3 explains the power assist system with construction of fuzzy inference for directional reasoning. In Chapter 4 presents the details about auto-tuning system of ANFIS and the simulation result for various operators. Finally, conclusion of this research and future works is summarized in Chapter 5.

Chapter 2

Description of the OMB

2.1 Introduction

An Omni-directional Mobile Bed (OMB) was designed and developed in author's laboratory. Because of its omni-directional ability, it is able to navigate smoothly in structured interior environments. This chapter describe the DDSS mechanism, the structure of the OMB and the hardwares as well as the kinematics of the OMB.

2.2 Differential Drive Steering System (DDSS)

A useful method for constructing a caster-drive wheel using a Differential-Drive Steering System (DDSS) was developed in author's laboratory [30],[31]. The DDSS outputs driving and steering velocities from two motors using differential gearing. Fig. 2.1 shows the principle of the DDSS. The differential gearing mechanism is realized by using five spur gears.The DDSS is a 2-input/2-output system without fixing any component. A and B are independently driven by two motors. C and D provide output torque. Fig. 2.2 shows the mechanism of the DDSS. Torques of two motors are transmitted to the DDSS by a bevel gear, D, which is fixed to the chassis E, provides the steering torque, and C, which leads to the driving wheel via the bevel gear, provides the driving torque. Let ω_A, ω_B, ω_C, $\acute{\omega_C}$ and ω_D be of the angular velocity of A, B, C, Ć and D in Fig. 2.1, and Z_A, Z_B, Z_C and $\acute{Z_C}$ be the number of teeth of A, B, C and Ć, respectively. When $\omega_D = 0$, the steering angular velocity ω_l becomes zero, and we obtain

$$\omega_A = \frac{\acute{Z_C}}{Z_A}\frac{Z_B}{Z_C}\omega_B = \frac{\acute{Z_C}}{Z_A}\omega_C \tag{2.1}$$

$$\omega_D = 0 \tag{2.2}$$

When $\omega_C - \omega_D = 0$, the driving angular velocity ω_w becomes zero because C does not rotate between A and B, and we obtain

$$-\omega_A = \omega_B = \omega_C (= \acute{\omega_C}) = \omega_D \tag{2.3}$$

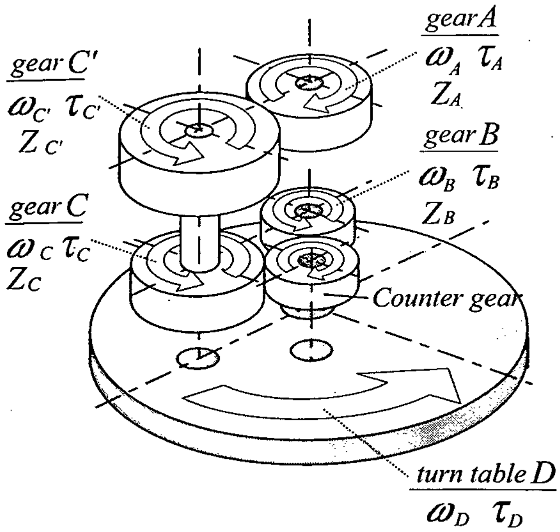

Fig. 2.1 Principle of the DDSS

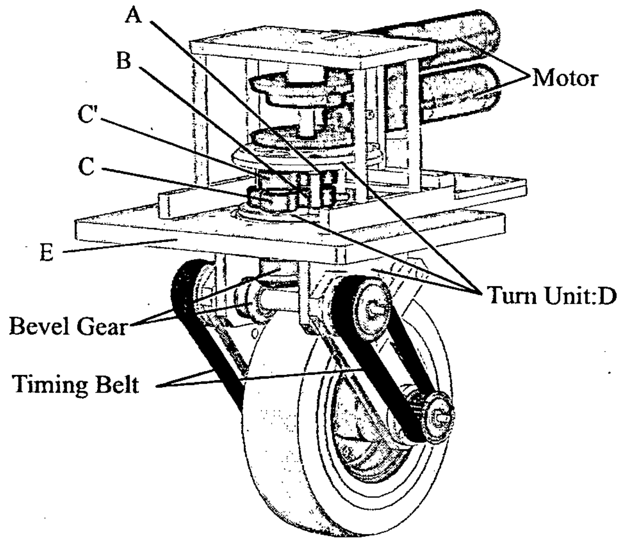

Fig. 2.2 Mechanism of the DDSS

The direct kinematic equation, which derives driving and steering output $u_w = [\omega_w, \omega_l]^T$ from motor input $u_P = [\omega_A, \omega_B]^T$, can be described as

$$u_w = \begin{bmatrix} \omega_C - \omega_D \\ \omega_D \end{bmatrix} = B_P u_P \tag{2.4}$$

where

$$B_P = \begin{bmatrix} \frac{Z_A Z_B}{Z_A Z_C + Z_B Z_C'} & \frac{Z_A Z_B}{Z_A Z_C + Z_B Z_C'} \\ -\frac{Z_A Z_C}{Z_A Z_C + Z_B Z_C'} & \frac{Z_B Z_C'}{Z_A Z_C + Z_B Z_C'} \end{bmatrix} \tag{2.5}$$

The inverse kinematic equation becomes

$$u_P = B_P^{-1} u_w \tag{2.6}$$

where

$$B_P^{-1} = \begin{bmatrix} \frac{Z_C'}{Z_A} & -1 \\ \frac{Z_C}{Z_B} & 1 \end{bmatrix} \tag{2.7}$$

2.3 Hardware of the OMB

Overview and specification of Omni-directional Mobile Bed (OMB) is shown in Fig. 2.3 and Table 2.3. The present system is comprised of Driving Unit by four omni-directional mobile mechanism with casters and Bed Unit with commercial electric reclining mechanism etc that will be explained in next section. The OMB handle and six-axis force sensor enable OMB to use in power-assist.

2.3.1 Driving unit

OMB is designed with DDSS casters. Fig. 2.4 show the driving platform of OMB. OMB is mainly divided by bed unit and driving unit. Bed unit consist of commercial bed, seat-up and leg-lift function, while driving unit consist of moving system, controller box and power assist handle.

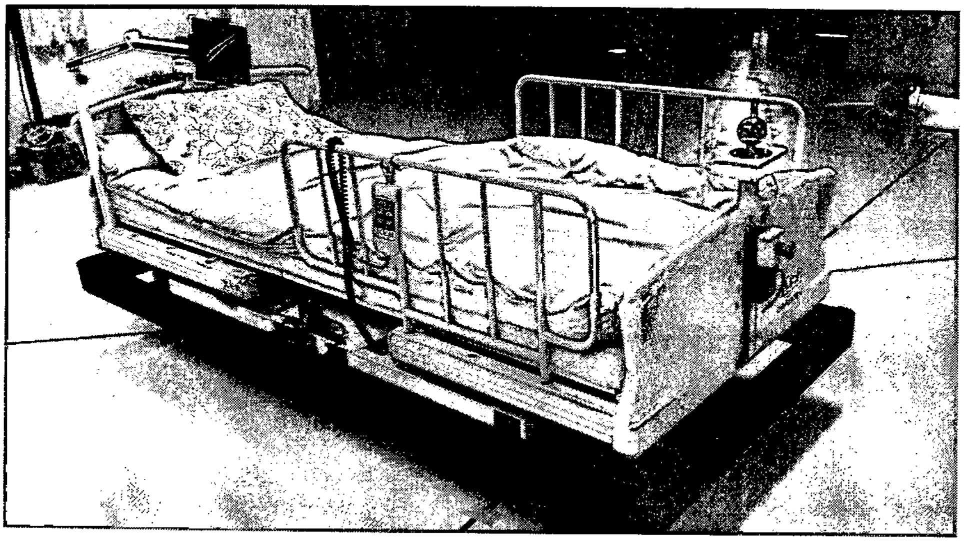

Fig. 2.3 Overview of Omni-directional Mobile Bed

Table 2.1 Specification of OMB

Size	Width	0.85[m]
	Depth	2.00[m]
	Height	0.90[m]
Weight		150[kg]
Mechanical characteristics	Maximum velocity	±3.00[km/h]
	Maximum angular velocity	±3.3[rad/s]
	Maximum acceleration	$\pm1.5[m/s^2]$
	Maximum angular acceleration	$\pm1.70[rad/s^2]$

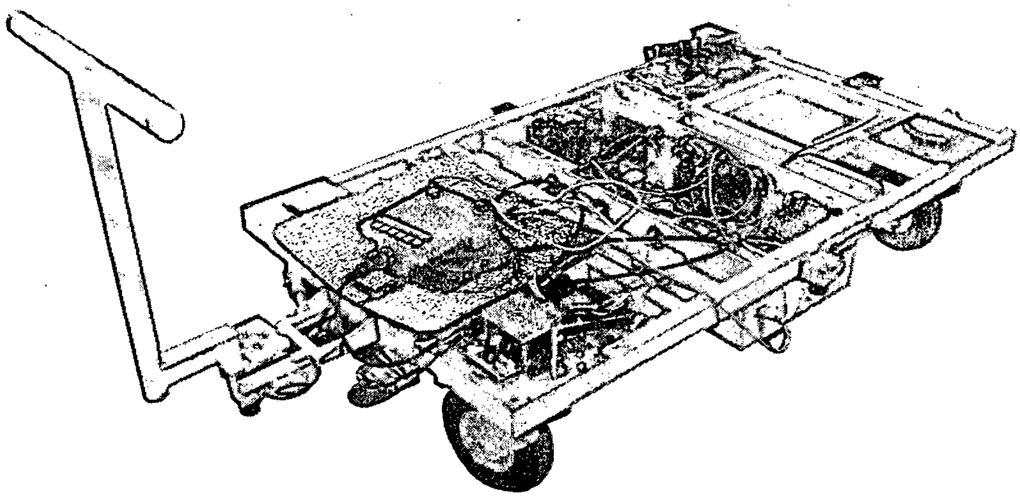

Fig. 2.4 Driving platform of OMB

Table 2.2 show the basic specification of DC servo motor, gear head, encoder, motor driver, bevel gear, spur gear, timing belt and others that used in driving system of OMB.

2.3.2 Seat-up driving unit

This equipment is for folding up the mattress on a bed in seating position form and also can lift up the legs. It is used for making a user to take a seating position posture at the time of a meal or other activities. Driving torque is able to support 80 [kg] load of adult in supine position to seating position. For safety of the patient, it can not be operated with turn-over driving unit in same time.

2.3.3 Turn-over driving unit

This device is for rotating the horizontal posture of the mattress on the bed. It is used to tilt the body posture of patient in rest time especially when the patient want to change his position. Driving torque is able to tilt maximum ± 10 [deg] and support 80 [kg] load of adult in supine position. For safety of the patient, it can not be operated with seat-up driving unit in same time.

2.3.4 Power assist handle and force sensor

Power assist system is utilized with respect to support the operational of the helper. The power assist system amplify the input force from helper, so it can be operated by small force. Thus, it is one of the solution to reduce the burden of helper.

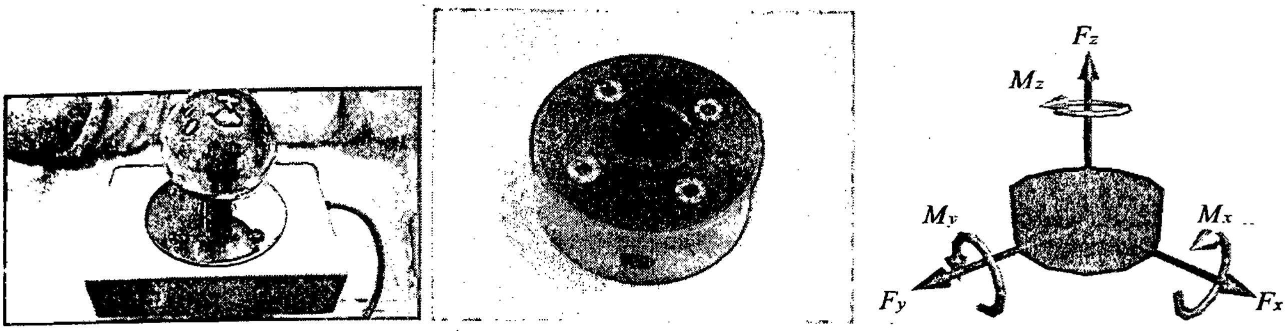

(a)Knob handle (b)Force sensor (c)Measurable axis

Fig. 2.5 Knob handle and 6-axis force sensor

In previous research, power assist handle was designed with two hand, but it was hard two operated on balancing by two hands especially when to move on lateral direction and rotation on center of gravity. The unbalance forces from right and left hand will lead the unintended direction. Therefore, the knob-handle is designed to replace the previous handle. The force of the operator is applied to this handle of the OMB shown in Fig. 2.5(a). This force is then measured by the 6-axis force sensor in Fig. 2.5(b) and Fig. 2.5(c). The specifications of the 6-axis force sensor used in this research are shown in Table 2.4.

2.3.5 Sensors and Tablet

One of the most important thing in development of welfare support equipment is to guarantee the safety of patients. For this purpose, various sensors are attached to the bed in order for detection, mapping, path-planning and avoiding collision of obstacles to support the operator while moving. This section will explain utilized sensors as shown in Fig. 2.6 and sensor model and maker is summarized in Table 2.4 , except for force sensor is described in section previous section.

Pressure sensor mat

Pressure sensor mat is a device for measuring the pressure distribution of patient on the bed as shown in Fig. 2.6(a). Pressure distribution information measured is used for analysis the condition of patient and able to used as interaction between human and bed. The size of sensor mat is W45 [cm] x H45 [cm], a size for wheelchair pressure sensor and combination more than two mats cover 90 percent of the bed area.

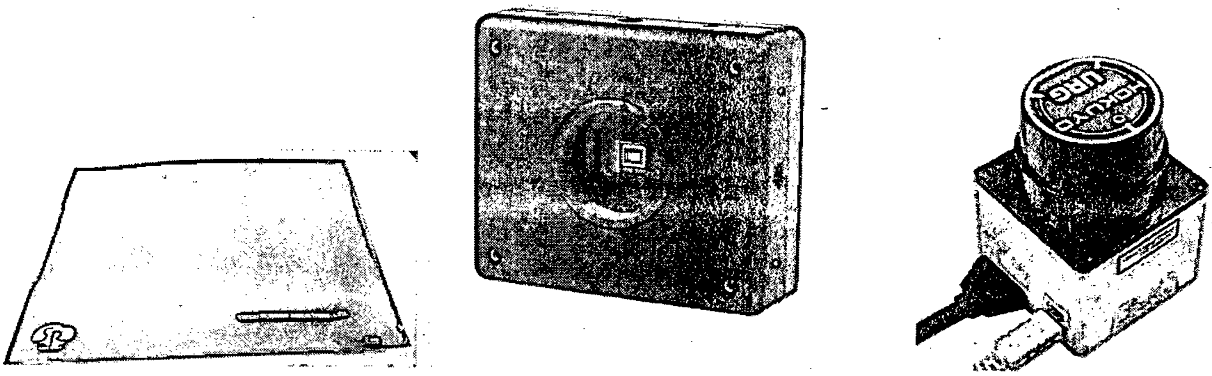

(a)Pressure sensor mat (b)Optical camera (c)Range sensor

Fig. 2.6 Utilized sensors for OMB

Bumper sensor

Bumper sensor detect the collision with the surrounding environment when there is contact to the sensor during the movement of the bed and absorb the stress caused by the collision. The bumper cover 90 percent of the bed frame and able to absorb more than 10 [mm] depth of shock. The width of the vertical direction of the bumper sensor is 10 [cm] and the withstand load for the shock is 0.1 [N/cm2].

Optical Camera

This device is is set up on every segment of the bed to obtain information from surrounding environment. Obtain video information is transfered to the tablet for view by the patient. The information also can be accessed in the integrated server in real time.

Laser range sensor

This device is set up on every segment of the bed for obtaining distance information of the surrounding environment. Distance information obtained is able to be processed as a two-dimensional map of the bed surround and is presented to the occupant through the tablet, also is used such as path planning of the mobile bed.

2.4 Kinematic model of OMB

Position and posture of bed is defined in the absolute coordinates as shown in Fig. 2.7. Here, center of steering in offset driving wheel is respectively $A(x_{va}, y_{va})$, $B(x_{vb}, y_{vb})$,$C(x_{vc}, y_{vc})$ and $D(x_{vd}, y_{vd})$. Each variable is defined respectively as follow and $i = a, b, c, d$.

$O_v(x_v, y_v)$: Center of bed in global coordinates[m]

θ_v : Bed posture(angle)[rad]

$\dot{x}_v$: x-directional velocity of bed[m/s]

$\dot{y}_v$: y-directional velocity of bed[m/s]

ω_v : rotational velocity of bed[rad/s]

(x_i, y_i) : global coordinates of steering center in each wheel[m]

$\dot{x}_i$: x-directional velocity in global coordinates in each wheel[m/s]

$\dot{y}_i$: y-directional velocity in global coordinates in each wheel[m/s]

$(x_{vi}, y_{vi}$: local coordinate of steering center of each wheel [m]

$\dot{x}_{vi}$: x-directional velocity in local coordinate of each whee[m/s]

$\dot{y}_{vi}$: y-directional velocity in local coordinate of each wheel[m/s]
O-XY is global coordinates, where Ov-XvYv is local coordinates in bed

Then, defining state vector of bed by $x = [x_v, y_v, \theta_v]^T$, and input vector to each wheel by $u = [x_a, y_a, x_b, y_b, x_c, y_c, x_d, y_d]^T$, the following kinematic model of mobile bed is derived ;

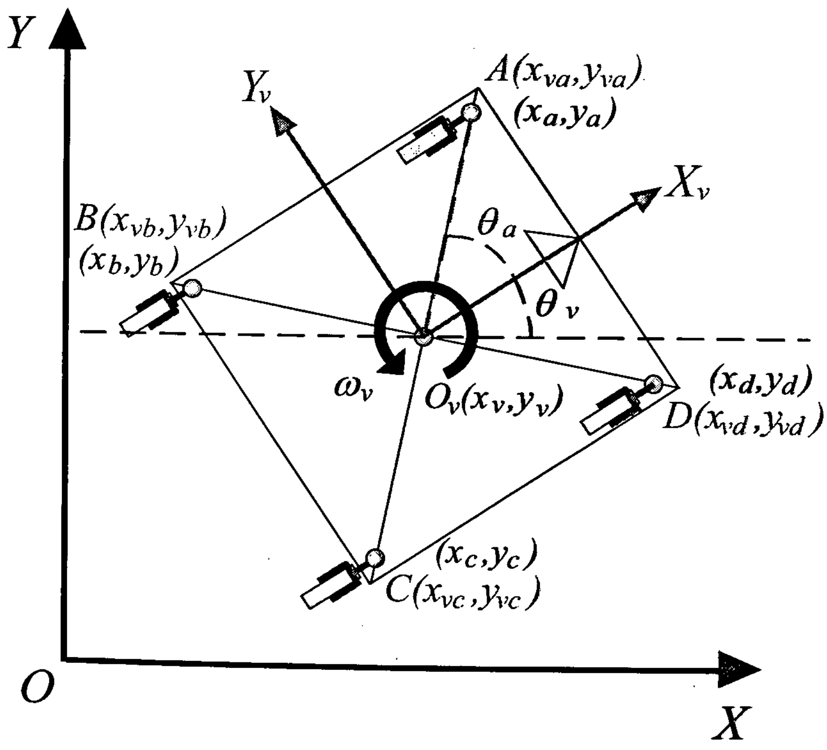

Fig. 2.7 Model of four-wheeled vehicle

$$\dot{x}_w = B_w u_w \tag{2.8}$$

$$\begin{bmatrix} \dot{x}_v \\ \dot{y}_v \\ \dot{\theta}_v \end{bmatrix} = \begin{bmatrix} \frac{1}{4} & 0 & -\frac{1}{4}(x_{va}\sin\theta_v + y_{va}\cos\theta_v) \\ 0 & \frac{1}{4} & \frac{1}{4}(x_{va}\cos\theta_v - y_{va}\sin\theta_v) \\ \frac{1}{4} & 0 & -\frac{1}{4}(x_{vb}\sin\theta_v + y_{vb}\cos\theta_v) \\ 0 & \frac{1}{4} & \frac{1}{4}(x_{vb}\cos\theta_v - y_{vb}\sin\theta_v) \\ \frac{1}{4} & 0 & -\frac{1}{4}(x_{vc}\sin\theta_v + y_{vc}\cos\theta_v) \\ 0 & \frac{1}{4} & \frac{1}{4}(x_{vc}\cos\theta_v - y_{vc}\sin\theta_v) \\ \frac{1}{4} & 0 & -\frac{1}{4}(x_{vd}\sin\theta_v + y_{vd}\cos\theta_v) \\ 0 & \frac{1}{4} & \frac{1}{4}(x_{vd}\cos\theta_v - y_{vd}\sin\theta_v) \end{bmatrix}^T \begin{bmatrix} \dot{x}_a \\ \dot{y}_a \\ \dot{x}_b \\ \dot{y}_b \\ \dot{x}_c \\ \dot{y}_c \\ \dot{x}_d \\ \dot{y}_d \end{bmatrix} \tag{2.9}$$

$$B_w = \begin{bmatrix} r\cos\theta_w & -l\sin\theta_w \\ r\sin\theta_w & l\cos\theta_w \end{bmatrix} \tag{2.10}$$

On the other hand, an inverse kinematic model is derived as follows;

$$u_w = B_w^{-1}\dot{x}_w \tag{2.11}$$

$$\begin{bmatrix} \dot{x}_a \\ \dot{y}_a \\ \dot{x}_b \\ \dot{y}_b \\ \dot{x}_c \\ \dot{y}_c \\ \dot{x}_d \\ \dot{y}_d \end{bmatrix} = \begin{bmatrix} 1 & 0 & -y_{va}\cos\theta_v - x_{va}\sin\theta_v \\ 0 & 1 & x_{va}\cos\theta_v - y_{va}\sin\theta_v \\ 1 & 0 & -y_{vb}\cos\theta_v - x_{vb}\sin\theta_v \\ 0 & 1 & x_{vb}\cos\theta_v - y_{vb}\sin\theta_v \\ 1 & 0 & -y_{vc}\cos\theta_v - x_{vc}\sin\theta_v \\ 0 & 1 & x_{vc}\cos\theta_v - y_{vc}\sin\theta_v \\ 1 & 0 & -y_{vd}\cos\theta_v - x_{vd}\sin\theta_v \\ 0 & 1 & x_{vd}\cos\theta_v - y_{vd}\sin\theta_v \end{bmatrix} \begin{bmatrix} \dot{x}_v \\ \dot{y}_v \\ \dot{\theta}_v \end{bmatrix} \tag{2.12}$$

$$B_w^{-1} = \begin{bmatrix} \frac{1}{r}\cos\theta_w & \frac{1}{r}\sin\theta_w \\ -\frac{1}{l}\sin\theta_w & \frac{1}{l}\cos\theta_w \end{bmatrix} \tag{2.13}$$

Block diagram of total system is shown in Fig. 2.8. Here, notation of r and e shows reference value and measured one respectively.

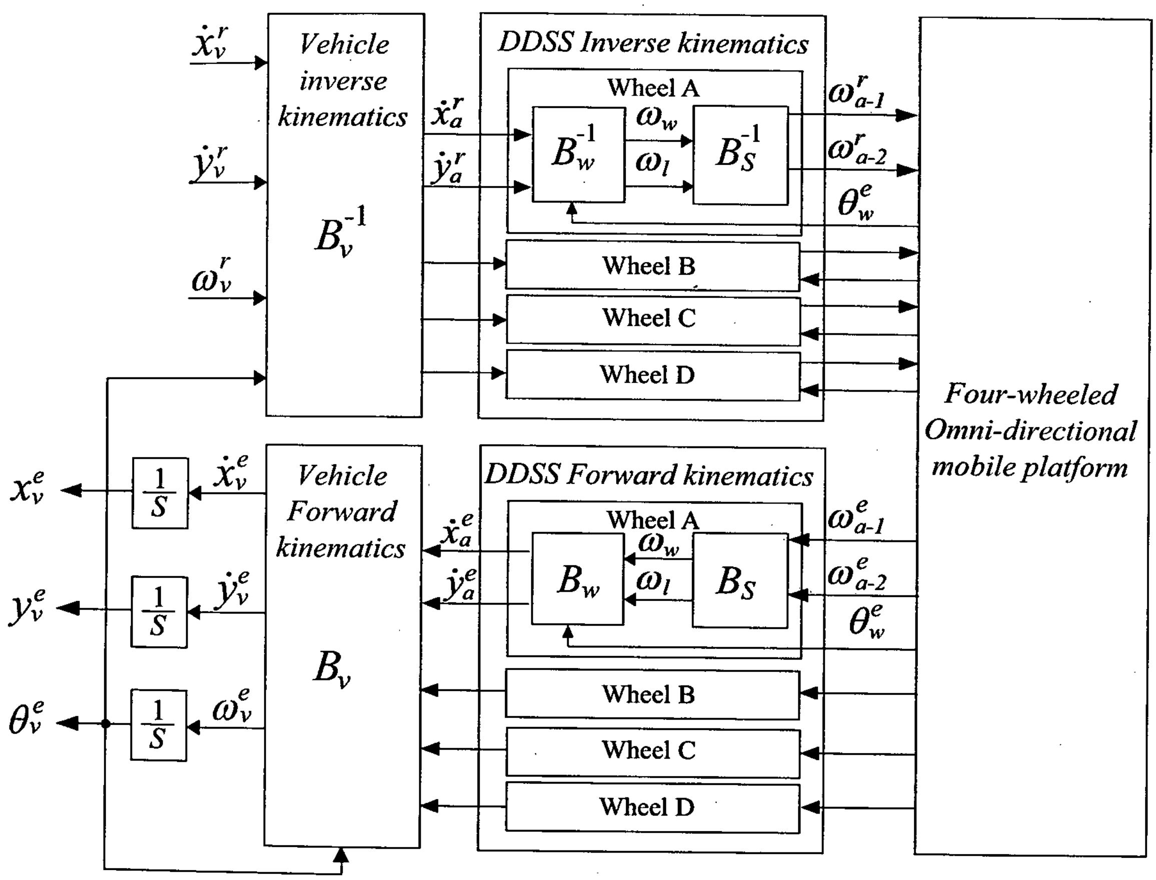

Fig. 2.8 Block diagram of four wheeled omni-directional mobile platform

Table 2.2 Specification of drive unit

Wheel	Maker	CHUBU-SANGYO Co.,Ltd.
	Model	GC2.50-4 (/駆動用)
	Diameter	208[mm]
	Width	62[mm]
	Maximum load	150[kg]
DC servo motor	Maker	maxon Japan CO.,Ltd.
	Model	RE40-148867
	Rated output	150[W]
	Rated notational velocity	7580[rpm]
	Nominal voltage	24[V]
	Maximum torque	191[mNm]
Gear head	Maker	maxon Japan CO.,Ltd.
	Model	GP42C-203119
	Gear ratio	15/1
Encoder	Maker	maxon Japan CO.,Ltd.
	Model	HEDL 5540-110514
	Resolution	500[pulse/rev]
	Power supply	± 5[V]
DC servo amplifier	Maker	maxon Japan CO.,Ltd.
	Model	EPOSP 24/5 & EPOS2 50/5-347717
	Supply voltage	11-50[V]
	Input voltage	± 10[V]
	Maximum output volatage	$0.9\times V_{CC}$[V]
	Maximum output current	10[A]
Absolute encoder	Maker	Omron CO.,Ltd.
	Model	E6J-AG1C
	Resolution	256[pulse/rev]
	Max. response frequency	20[kHz]
	Power supply voltage	5[V]
	Output code	Gray code
Spur gear	Maker	KOHARA GEAR INDUSTRY CO., Ltd.
	Model	Z_A : SS1.5-20, Z_B : SS1.5-18 $\acute{Z}_C$: SS1.5-30, Z_C : SS1.5-27
	Gear ratio$(Z_A/\acute{Z}_C = Z_B/Z_C)$	2/3
Bevel gear	Maker	KOHARA GEAR INDUSTRY CO., Ltd.
	Model	SB1.5-4515 & SB1.5-1545
	Gear ratio	1/3
	Model	MM2-20
	Gear ratio	1/1
Timing pulley	Maker	Tsubakimoto Chain CO.
	Model	HTPA-K24S5M-100 & K30S5M-100
	Gear ratio	4/5

Table 2.3 Specification of force sensor

Maker	NITTA CORP.
Model	IFS-67M25A25-140-ANA
Capacity of F_x, F_y	± 100 [N]
Capacity of F_z	± 200 [N]
Capacity of M_x-M_z	± 7[Nm]
Diameter	67 [mm]
Height	25 [mm]
Mass	0.18 [kg]
Input voltage	± 7-15 [V]
Output voltage	± 5 [V]

Table 2.4 List of devices

Device name	Model	Maker
Bed pressure mat	SR Softvision	Tokai Rubber
Wheelchair pressure mat	SR Softvision	Tokai Rubber
Optical Camera	Dragonfly2	Pointgray
Range sensor	URG-04LX	Hokuyo Electric
Tablet	Xperia Tablet Z	Sony Mobile Comm.
Driving control device	PC104	Advantech
Recognition Integrated device	Thinkpad X230	Lenovo
External computer	Think Station C30	Lenovo

Chapter 3

Power Assist Control with Direction Estimator

3.1 Power-assist controller

When operating OMB with patient, the total load can reach about 200[kg], and it is hard to operate and very dangerous particularly in hospital and welfare facility which support the elder and disable people. Therefore, in order to reduce the burden of the operator and provide safety transferring of patient, power assist is applied to the OMB.

When force $F = \begin{bmatrix} f_x & f_y & m_z \end{bmatrix}^T$ is applied to the handle by the operator, the force is converted to reference velocity V_{OMB} of OMB. Power-assisted method is used a control method for generating a reference velocity value proportional to the force. Therefore, though the load of passenger is change whether become bigger or smaller, the output velocity is responded only to the input force and the operator can operate with the same amount of force. In addition, it is advantageous when there is no input force on slope condition the velocity will become zero, the wheel is locked and will not slip because there is no affect from gravity force.

When applied force is converted to velocity of OMB, from Newton's second law, $m\ddot{x} = f$ it is understood that input force is corresponds to the acceleration. When human being is walking, the step cycle and up-and-down motion inevitably generate vibration and hand shake. Therefore, since the vibration while walking need to be reduced, it can be said that the power assist controller requires an integral element. Moreover, in order to avoid the OMB is keep running even when the hands is lifted, the viscosity characteristic is need to the clause proportional to acceleration, that is velocity. Therefore, the OMB will stop automatically once the operator release the handle.

Therefore, here from input force is $f(t)$, mass is m, viscosity coefficient is c, displacement is $x(t)$, Eq. 3.1 can be obtained.

$$f(t) = m\ddot{x}(t) + c\dot{x}(t) \tag{3.1}$$

due to velocity control, so $v = \dot{x}$

$$f(t) = m\dot{v}(t) + cv(t) \tag{3.2}$$

is obtained, Eq. 3.2 is transformed to Laplace transform. Then, Eq. 3.3 is obtained.

$$F(s) = msV(s) + cV(s) \tag{3.3}$$

then, Eq. 3.3 is modified to,

$$V(s) = \frac{\frac{1}{c}}{\frac{m}{c}s + 1} \tag{3.4}$$

is understood as first lag order system. Then, Eq. 3.4 can be modified to Eq. 3.5 as

$$V(s) = \frac{K}{Ts + 1}F(s) \tag{3.5}$$

From parameters of gain K and time constant T the controller can be designed. Therefore, the magnitude of velocity of OMB that generated from input force can be changed, by changing the gain K. Likewise, we can change the velocity response that generate velocity of OMB from input force, by changing the time constant T.

From the above, from X-axis force f_x[N] to X-axis velocity v_x^P[m/s], from Y-axis force f_y[N] to Y-axis velocity v_y^P[m/s], from Z-axis moment m_z[Nm] to Z-axis angle velocity ω^P[rad/s] can be obtained as next equation

$$\begin{bmatrix} V_x^P(s) \\ V_y^P(s) \\ \Omega^P(s) \end{bmatrix} = \begin{bmatrix} \frac{K_{vx}}{T_{vx}s+1} & 0 & 0 \\ 0 & \frac{K_{vy}}{T_{vy}s+1} & 0 \\ 0 & 0 & \frac{K_\omega}{T_\omega s+1} \end{bmatrix} \begin{bmatrix} F_x(s) \\ F_y(s) \\ M(s) \end{bmatrix} \tag{3.6}$$

Here, K_{vx} : gain controller of X-axis, T_{vx} : time constant of controller of X-axis, K_{vy} : gain controller of Y-axis, T_{vy} : time constant of controller of Y-axis, K_ω : gain controller of Z-axis, T_ω : time constant of Z-axis.

3.2 A skill-assist system by using a navigation direction estimator

When the operator tries to rotate the OMB around its gravity center, the OMB begins to slide and the radius of rotation becomes very large, as shown in Fig. 3.1.

Rotation around the gravity center is very difficult because the large size, rectangle-shaped of OMB and also influenced by any force that acts in the lateral direction, as shown. A survey was conducted among various operators trying to discover some relationships in the way they realized forwards-backwards, lateral, and rotational movements. The goal of the survey was to find general rules that drew a relationship between the three described motions. Though it

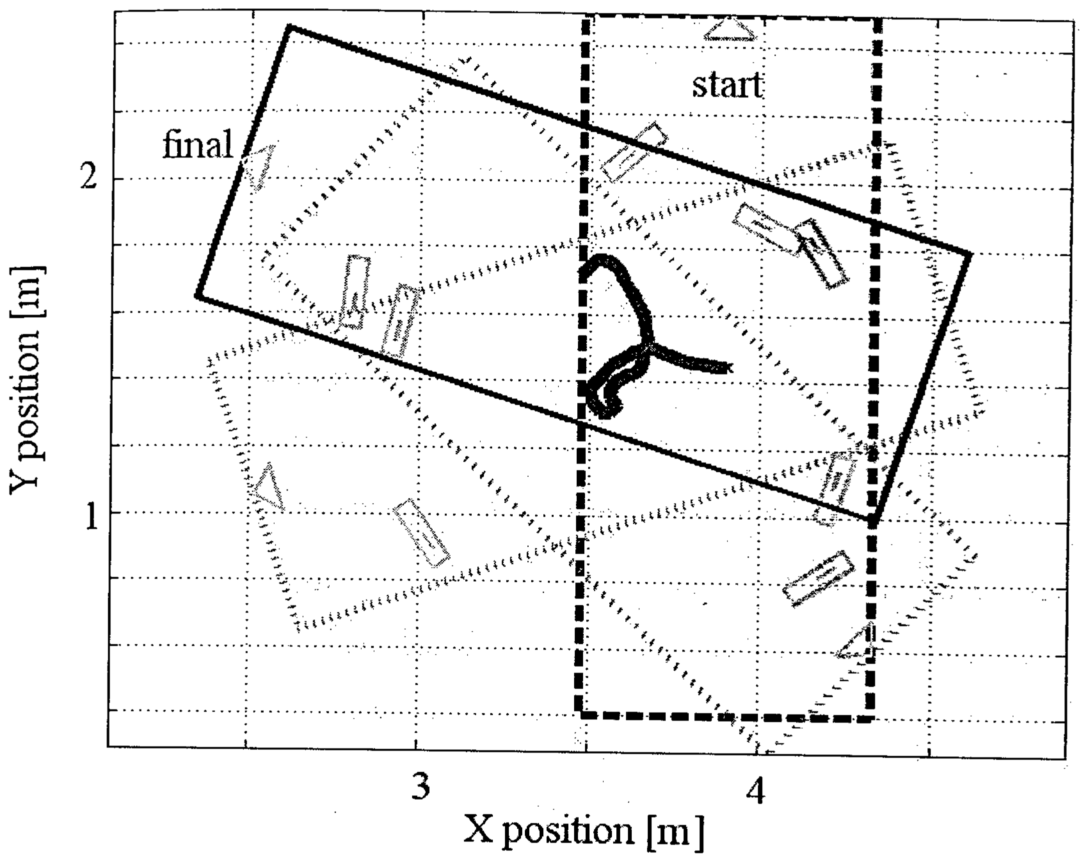

Fig. 3.1 A case of rotational movement of OMB in counter-clockwise (CCW) direction, when just power-assist is used

was impossible to find general rules that explained all cases, a relationship was found between lateral and rotational movements. It was found that if the movement in the forward or backward direction is not considered, when most of the operators want to:

I) rotate in a clockwise (CW) direction, in addition to the rotational momentum they use some force in the lateral left direction.

II) rotate in a counter-clockwise (CCW) direction, in addition to the rotational momentum they use some force in the lateral right direction.

III) move in a lateral right direction, in addition to the lateral force they use some momentum in the CW direction

IV) move in a lateral left direction, in addition to the lateral force they use some momentum in the CCW direction

According to the traditional convention, CCW rotation is considered to be produced by a positive angular velocity $\omega > 0$, rotation in CW direction is considered to be produced by a negative angular velocity $\omega < 0$, lateral movement to the right is considered to be produced by a positive lateral velocity $Vy > 0$ and lateral movement to the left is considered to be produced by a negative lateral velocity $Vy < 0$.

Sometimes there is neither rotational movement nor lateral movement. Thus, for completeness, two more variables: $\omega \approx 0$, expressing the case of no rotation, and $Vy \approx 0$, expressing the case of no lateral movement, must be included.

Following what has been established in the previous paragraphs, it is possible to construct the following table:

Table 3.1 Empirical rules

1	If	$\omega < 0$ and $Vy < 0$,	then	rotational movement in the CW direction
2	If	$\omega > 0$ and $Vy > 0$,	then	rotational movement in the CCW direction
3	If	$Vy > 0$ and $\omega < 0$,	then	lateral movement to the right
4	If	$Vy < 0$ and $\omega > 0$,	then	lateral movement to the left
5	If	$\omega < 0$ and $Vy \approx 0$,	then	rotational movement in CW direction
6	If	$\omega > 0$ and $Vy \approx 0$,	then	rotational movement in CCW direction
7	If	$Vy > 0$ and $\omega \approx 0$,	then	lateral movement to the right
8	If	$Vy < 0$ and $\omega \approx 0$,	then	lateral movement to the left
9	If	$Vy \approx 0$ and $\omega \approx 0$,	then	no movement

Table 3.2 First fuzzy inference system

1	If	$\omega < 0$ and $Vy < 0$,	then	$\omega < 0$
2	If	$\omega > 0$ and $Vy > 0$,	then	$\omega > 0$
3	If	$Vy > 0$ and $\omega < 0$,	then	$Vy > 0$
4	If	$Vy < 0$ and $\omega > 0$,	then	$Vy < 0$
5	If	$\omega < 0$ and $Vy \approx 0$,	then	$\omega < 0$
6	If	$\omega > 0$ and $Vy \approx 0$,	then	$\omega > 0$
7	If	$Vy > 0$ and $\omega \approx 0$,	then	$Vy > 0$
8	If	$Vy < 0$ and $\omega \approx 0$,	then	$Vy < 0$
9	If	$Vy \approx 0$ and $\omega \approx 0$,	then	0

The system shown in Table 3.2 can be appropriately represented by a Takagi-Sugeno-Kang fuzzy model[32],[33], with appropriate membership functions for the input, and the output being a function of the inputs, such as:

$$y_i = A_i \times Vy_j + B_i \times \omega_j + C_i \tag{3.7}$$

where y_i represents the output function, i is a sub-index that indicates the rule to which the coefficients correspond, and the sub-index j can take any value in the set $\{N, Z, P\}$.

Then, by rearranging the rules of Table 3.2 and using the output function y_i, the system described in Table 3.2 becomes as shown in Table 3.3.

Lateral velocity $\boldsymbol{Vy}$ is in the range [-1.0 ~ 1.0], and angular velocity ω is in the range [-1.0 ~ 1.0]. The units of $\boldsymbol{Vy}$ and ω are [m/s] and [rad/s], respectively. After much trial and error, it was found that the more appropriate values for $Vy < 0$, $Vy \approx 0$, $Vy > 0$, $\omega < 0$, $\omega \approx 0$, and $\omega > 0$ correspond to the following ranges:

The functions used for the partitions of the total range of $\boldsymbol{Vy}$ and ω are called ***dsigmoidal*** functions, and are defined as the difference of two sigmoidal functions. That is, if Eq. (3.8) is a sigmoidal function, with input data $\boldsymbol{x}$, and parameters $\boldsymbol{a}$ and $\boldsymbol{c}$, where $\boldsymbol{a}$ defines the inclination of the curve in the crossover point $\boldsymbol{c}$. Crossover points are defined [35] as the points in which $\mu = 0.5$. Depending on the sign of the parameter $\boldsymbol{a}$, the sigmoidal membership function is inherently open to the right or to the left (if $\boldsymbol{a}$ is positive, the function is open to the right, and if $\boldsymbol{a}$ is negative the function is open to the left).

Table 3.3 Takagi-Sugeno-Kang fuzzy model

R	Antecedent			Consequent
1	If	$Vy < 0$ and $\omega < 0$,	then	$y_1 = A_1 \times Vy_N + B_1 \times \omega_N + C_1$
2	If	$Vy \approx 0$ and $\omega < 0$,	then	$y_2 = A_2 \times Vy_Z + B_2 \times \omega_N + C_2$
3	If	$Vy > 0$ and $\omega < 0$,	then	$y_3 = A_3 \times Vy_P + B_3 \times \omega_N + C_3$
4	If	$Vy < 0$ and $\omega \approx 0$,	then	$y_4 = A_4 \times Vy_N + B_4 \times \omega_Z + C_4$
5	If	$Vy \approx 0$ and $\omega \approx 0$,	then	$y_5 = A_5 \times Vy_Z + B_5 \times \omega_Z + C_5$
6	If	$Vy > 0$ and $\omega \approx 0$,	then	$y_6 = A_6 \times Vy_P + B_6 \times \omega_Z + C_6$
7	If	$Vy < 0$ and $\omega > 0$,	then	$y_7 = A_7 \times Vy_N + B_7 \times \omega_P + C_7$
8	If	$Vy \approx 0$ and $\omega > 0$,	then	$y_8 = A_8 \times Vy_Z + B_8 \times \omega_P + C_8$
9	If	$Vy > 0$ and $\omega > 0$,	then	$y_9 = A_9 \times Vy_P + B_9 \times \omega_P + C_9$

Table 3.4 Range of velocities

$\boldsymbol{Vy}$	Range	ω	Range
$Vy < 0$	[-1.0 ~ -0.05)	$\omega < 0$	[-1.0 ~ -0.1)
$Vy \approx 0$	[-0.05 ~ 0.05]	$\omega \approx 0$	[-0.1 ~ 0.1]
$Vy > 0$	(0.05 ~ 1.0]	$\omega > 0$	(0.1 ~ 1.0]

$$f(x, a, c) = \frac{1}{1 + e^{-a(x-c)}} \tag{3.8}$$